Supplementary information

Ion-induced bias in Ag_2S luminescent nanothermometers

M. París Ogáyar[a], D. Mendez-Gonzalez[b, c], I. Zabala Gutierrez[c], Á. Artiga[a], J. Rubio-Retama[b, c], O. G. Calderón[d], S. Melle[d], A. Serrano[e], A. Espinosa[f], D. Jaque[a, b, g, h*] and R. Marin[a, g, h*]

[a] NanoBIG, Departamento de Física de Materiales, Facultad de Ciencias, Universidad Autónoma de Madrid, C/Francisco Tomás y Valiente 7, Madrid, Spain
[b] Nanobiology Group, Instituto Ramón y Cajal de Investigación Sanitaria (IRYCIS), Ctra. De Colmenar Viejo, Km. 9100, Madrid, Spain
[c] Department of Chemistry in Pharmaceutical Sciences Faculty of Pharmacy Complutense University of Madrid Plaza Ramon y Cajal 2, Madrid 28040, Spain
[d] Department of Optics Faculty of Optics and Optometry, Complutense University of Madrid, Arcos de Jalón 118, Madrid E-28037, Spain
[e] Instituto de Cerámica y Vidrio| CSIC. Campus de Cantoblanco, C. Kelsen, 5, 28049 Madrid, Spain.
[f] Instituto de Ciencia de Materiales de Madrid | CSIC. Campus de Cantoblanco, C. Sor Juana Inés de la Cruz, 3, 28049 Madrid, Spain
[g] Institute for Advanced Research in Chemical Sciences (IAdChem), Universidad Autónoma de Madrid, Madrid 28049, Spain
[h] Instituto Nicolás Cabrera, Universidad Autónoma de Madrid, 28049 Madrid, Spain

Table of contents

(I) Materials and methods

(I.I) Materials

(a) Chemicals

Sodium diethyldithiocarbamate (NaDDTC) (ACS reagent grade), silver nitrate (99.9%), oleylamine (70%) (OLA), 1-dodecanethiol (≤98%) (DDT), were purchased from Sigma-Aldrich (Merck). Heterobifunctional HS-PEG(2kDa)-Methoxy was purchased from Rapp polymere GmbH. Chloroform ($CHCl_3$) (99.6%) and ethanol absolute pure (99.8%) were purchased from PanReac AppliChem. n-Hexane (99%) was purchased from labkem. Synomag®-D (10 mg/mL aqueous dispersions; dextran NH_2 surface coating; 50 nm hydrodynamic diameter), were acquired from ©Micromod Partikeltechnologie GmbH and used as received.

(I.II) Methods

(a) Synthesis of Ag_2S NPs

The synthesis of the NPs was performed following a previously reported method[1]. Ag_2S NPs were produced through the thermal decomposition of silver diethyldithiocarbamate (AgDDTC), used as precursor. This reactant was previously prepared by the reaction between 0.025 mmol of $AgNO_3$ and 0.025 mmol of NaDDTC, separately pre-dissolved in 200 mL of Milli-Q water. The slowly addition of the NaDDTC solution above the $AgNO_3$ solution produced a yellow precipitate (AgDDTC). The product was filtered under vacuum, dried at 60ºC and stored in a desiccator protected from light for further use. The production of Ag_2S NPs was carried out by adding 25 mg of AgDDTC (0.1 mmol), 2.5 mL of DDT (10.4 mmol) and 2.5 mL of OLA (7.6 mmol) into a two-neck round-bottom flask at room temperature. The mixture was first sonicated under vacuum for 10 min to remove air and residual water. Next, it was heated up to 185 °C at a heating rate of 20 °C/min under nitrogen atmosphere and slow magnetic stirring. The reaction was kept for 1 h, and then it was let to cool down naturally. The synthesized NPs were destabilized with 10 mL of ethanol and collected by centrifugation at 10000 G for 10 min; this process was repeated twice. Finally, the pellet formed by the precipitated NPs was dispersed in $CHCl_3$ at a concentration of 1 mg/mL and stored at 4 °C.

(b) Surface functionalization of Ag_2S NPs with HS-PEG-OMe

Firstly, 3 mL of Ag_2S NPs dispersion (1 mg/mL) were added to a vial containing 15 mg of HS-PEG-OMe (Mw = 2kDa) and the resulting mixture was incubated in an orbital shaker for 1h. After this, the dispersion was bath-sonicated until a change in its appearance was observed (from a turbid and colloidally unstable dispersion to a product with low scattering, high colloidal stability, and bright color), typically after 10 min of ultrasonication. This dispersion was then destabilized by the addition of 6 mL of hexane and centrifuged at 2000 G for 1 min. The resulting pellet was redispersed in 1.2 mL of ethanol by hand shaking and eventually sonicating during ~15 sec. After this, 2.8 mL of di-H_2O were added dropwise while sonicating the vial. The dispersion was next transferred to a 10 mL round bottom flask, and the organic solvent traces were removed using a rotary evaporator. The dispersion was finally purified using an Amicon® Ultra centrifuge filter

(50k). After 3 cycles of centrifugation (5 min, 14000 G) and redispersion in di-H_2O, the resulting Ag_2S-PEG-OMe NPs were dispersed to a final volume of 40 µL of di-H_2O and stored at 4 °C.

(c) Steady state luminescence

For steady state luminescence measurements we used a single mode fiber 808 nm laser diode as excitation (Lumics BTF14). The luminescence was acquired with a NIR Quest spectrometer (900-2500 nm wavelength) from Ocean Insight. An 850 nm long-pass filter (FELH0850 Thorlabs) was used to remove the laser contribution. The cuvette was placed in an air-cooled Qpod 3e (Quantum Northwest) for temperature control.

(d) Thermal measurements

Local temperature increase within the Ag_2S NPs (0.5 mg/mL) and γ-Fe_2O_3 NFs (9.5 mg/mL) mixture was probed with a digital thermocouple type-K (0.1 ºC sensitivity) in a 3 x 3 mm optical path cuvette and upon 808 nm continuous wave laser excitation (P = 200 mW).

(e) Luminescence lifetime measurements

Luminescence decay curves were performed using a Time-Correlated Single Photon Counting Timeharp 260 system (PicoQuant) equipped with an 82.4 ps pulse diode laser with 634.3 nm excitation (EPL-640 form Edinburgh Instruments). An 850 nm long-pass filter (FELH0850 Thorlabs) was used to remove the laser contribution. The decay broadband emission were acquired with a fixed temperature of 20 ºC (air-cooled Qpod 3e from Quantum Northwest).

(f) Colorimetric essays

Two different 200 µL dispersions of NFs were prepared for the colorimetric essays, one was continuously irradiated with an 808 nm wave laser (P = 200 mW) during 3 h and the other was used as control. Both dispersions were purified using an Amicon 50k centrifuge filter resuspending 150 µL of the filtered NFs in 530 µL distilled water. Dispersions were stirred and heated up to 40 ºC with 160 µL of Hydroxylamine Hydrochloride 10 % to facilitate the reduction of ion Fe^{3+} to Fe^{2+}. Finally, 160 µL of 1,10-Phenanthroline 0.3% was added to conform the characteristic orange-red complex ion. The absorption spectra of the final solutions were acquired with a Varian Cary 5000 spectrophotometer and 1 x 1 cm optical paths cuvettes.

(g) Photocatalyst performance

30 µl of super-concentrated NFs [42 mg/mL] were mixed in 100 µL RhB aqueous solution [12.25 µM]. Under NIR illumination with an 808 nm wave laser (P = 200 mW), 20 µl aliquot was collected after certain illumination time (t = 0, 30 and 60 min). After the collection, the 20 µL of RhB + NFs mixture was diluted in 40 µL of distilled water. After centrifugation, 20 µl of RhB supernatant was diluted until 60 µL and the absorbance was monitored with a Plate Reader (SpectraMax Mini Molecular Devices). The degradation of RhB upon 808 nm irradiation was also evaluated by diluting the 20 µL aliquots from the irradiated sample in 60 µL of distilled water.

(h) X-ray absorption spectroscopy (XAS)

X-ray absorption spectroscopy (XAS) measurements were performed at the Ag K-edge (25514 eV) at BM30 beamline of the European Synchrotron Radiation Facility (The ESRF) in Grenoble (France). Experiments were performed on dry drops in fluorescence mode and at room temperature, with an average accumulation of 5 scan acquisitions per sample in order to improve signal-to-noise ratio. Investigations were carried out both in X-ray absorption near edge structure (XANES) and extended X-ray absorption fine structure (EXAFS) regions. Ag metallic foil was measured and used to calibrate the energy. The XAS analysis was performed using the Athena and Artemis software.[2]

(II) Results

(S1) Characterization of Ag_2S LNThs and γ-Fe_2O_3 NFs

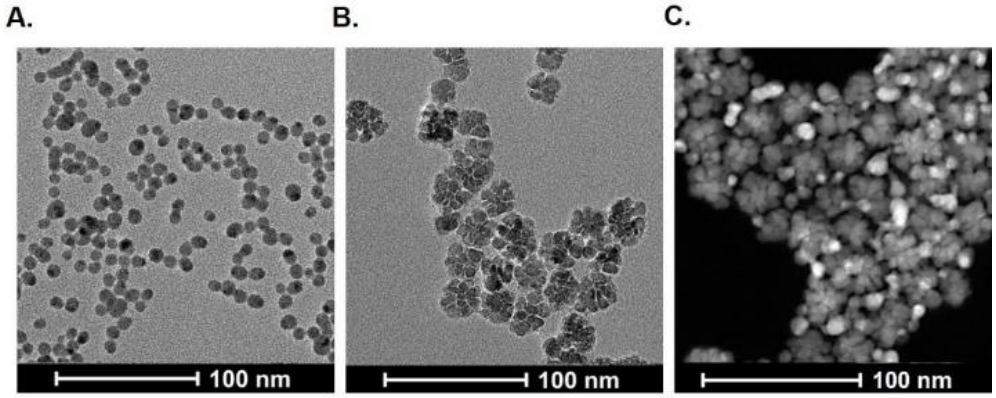

Figure S1. Characterization of Ag_2S LNThs and γ-Fe_2O_3 NFs. (A) TEM image of synthesized Ag_2S LNThs. (B) TEM image of γ-Fe_2O_3 NFs. (C) HAADF images in TEM of Ag_2S LNThs (0.5 mg/mL) and γ-Fe_2O_3 NFs (9.75 mg/mL) mixture. Brighter parts correspond to Ag.

In a standard mixture for performed experiments -Ag_2S LNThs (0.5 mg/mL) and γ-Fe_2O_3 NFs (9.75 mg/mL)-, we estimated that there are 3 Ag_2S LNThs per each NF.

1. Ag_2S LNThs with 4.5 nm radius, a density of 7.23 g/cm^3 and concentrated 0.5 mg/mL in 100 µL of deionized water: $1.81 \cdot 10^{13}$ particles.
2. γ-Fe_2O_3 NFs (9.75 mg/mL) in 100 µL of deionized water. Commercial nanoflowers with $6.1 \cdot 10^{13}$ particles/mL (data acquiered from ©Micromod Partikeltechnologie): $5.95 \cdot 10^{12}$ particles.

(S2) Photothermal heating of Ag_2S LNThs and γ-Fe_2O_3 NFs

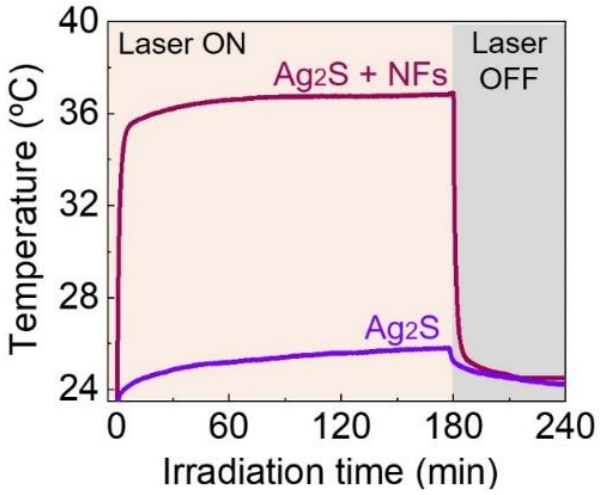

Figure S2. Heating of Ag_2S LNThs alone (0.5 mg/mL) and mixture of Ag_2S LNThs (0.5 mg/mL) and γ-Fe_2O_3 NFs (9.75 mg/mL) during 3h of irradiation. Global temperature of the solution was recorded with a thermocouple.

(S3) Optical density spectra of Ag_2S LNThs and γ-Fe_2O_3 NFs (500-850 nm)

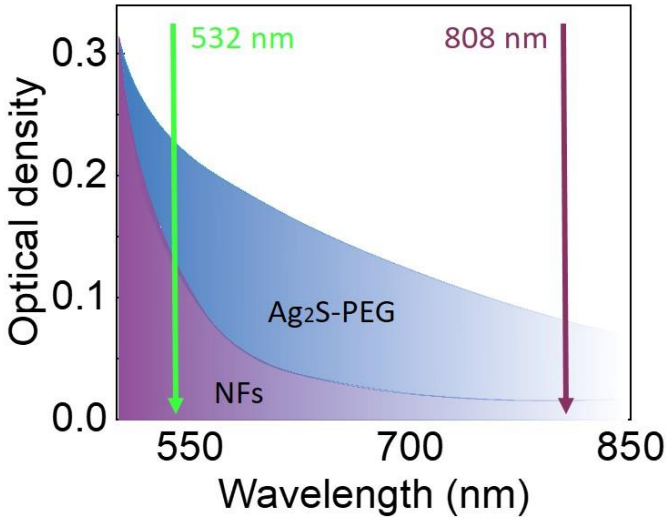

Figure S3. Optical density spectrum of Ag_2S LNThs (0.15 mg/mL) and γ-Fe_2O_3 NFs (0.15 mg/mL). Absorbance increases for both nanoparticles in the visible range (comparison of absorbance at 532 and 808 nm).

(S4) Chemical reaction process to detect Fe ions and corresponding calibration

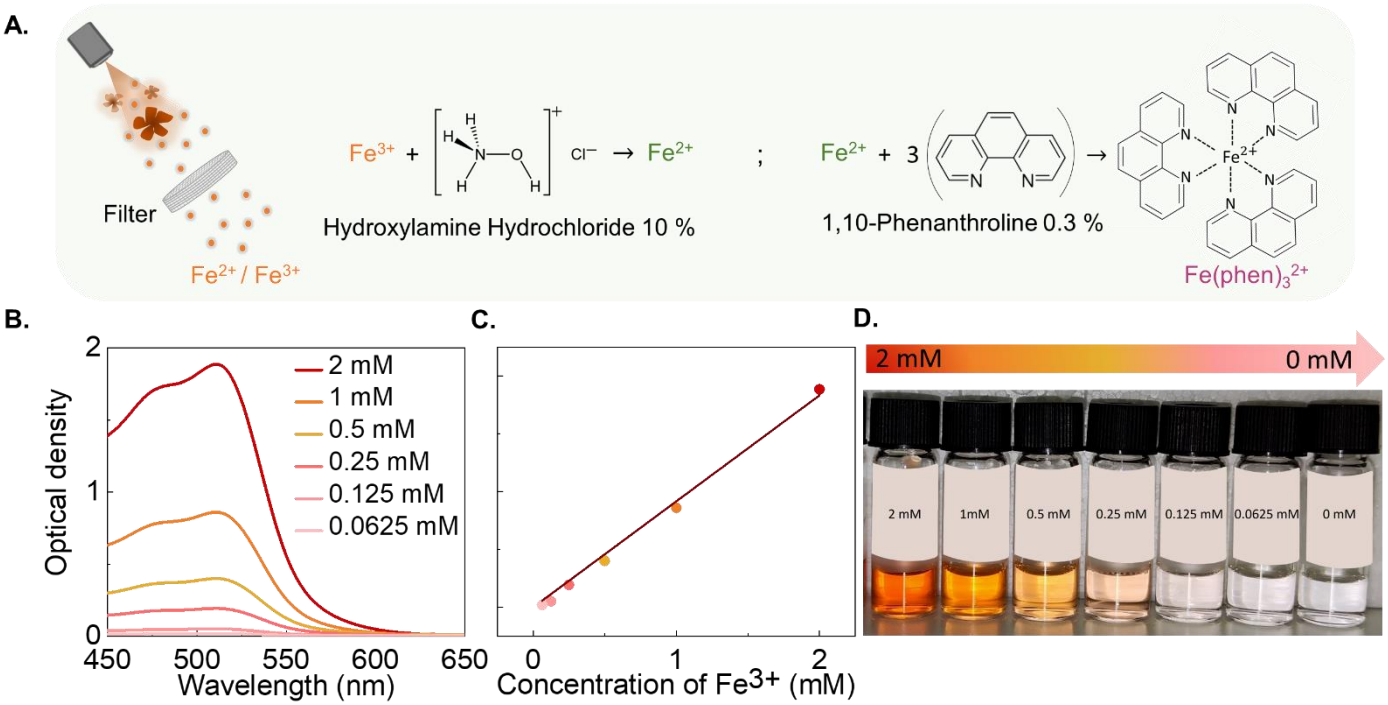

Figure S4. (A) Chemical reaction process to detect Fe ion. Firstly, irradiated NFs (or non-irradiated for control) were filtered. Secondly, an addition of Hydroxylamine Hydrochloride was used to reduce ion Fe^{3+} to Fe^{2+} Finally, 1,10-Phenanthroline was employed to conform the characteristic orange-red complex ion. (B) Spectral profile for different concentration of Fe in solution (C) Calibration curves with linear dependence taking the maximum value of each spectrum (510 nm). (D) Solution color images varying the concentration of Fe ions (2 mM to 0 mM).

By the maximum value of each spectrum in **Figure S4B** (around 510 nm) we obtained the calibration curves with a linear dependence and Pearson correlation coefficient close to 1 (**Figure S4C**). The linear equation is the following:

$$y = 0.91709x$$ (*y* is the optical density and *x* the Fe concentration)

Subtracting the scattering part of **Figure 4** to the spectrum corresponding to Fe ions in solution, we estimated that for an optical density of 0.0022, the Fe ion concentration present in the solution is 2 µM.

(S5) Photocatalytic effects: Rhodamine assay

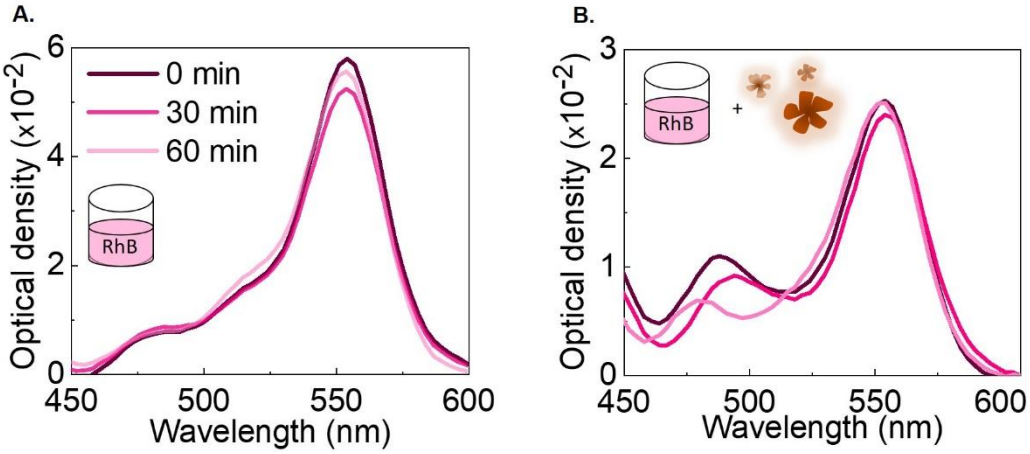

Figure S5. Photocatalytic effects (A) Photodegradation of Rhodamine B (RhB) alone collecting sample after different irradiating times (0, 30 and 60 min) at 808 nm excitation (200 mW). (B) Photodegradation of RhB with NFs collecting sample and filtrating after different irradiating times (0, 30 and 60 min) at 808 nm excitation. Bands found around 475 and 500 nm could be associated to some NF contribution since centrifugation process is not 100 % effective.

(S6) EDX elemental maps

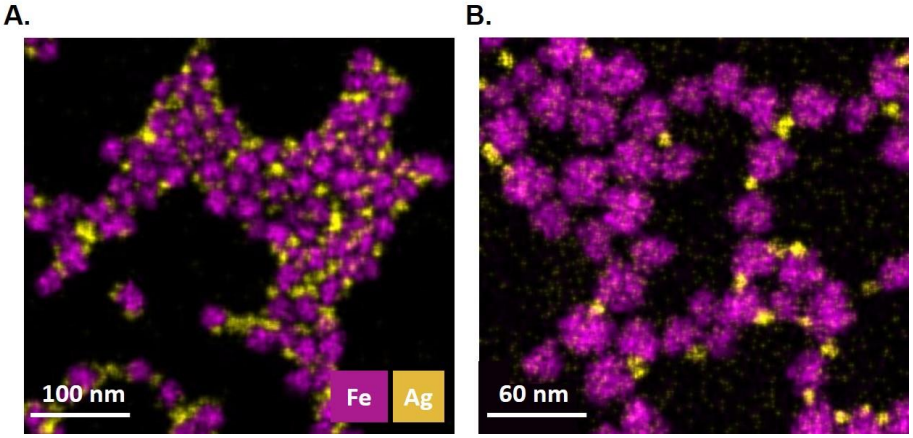

Figure S6. Energy dispersive X-Ray spectrometry (EDX) elemental maps of Fe (magenta) and Ag (yellow) of (A) Non irradiated Ag_2S LNThs (0.5 mg/mL) + γ-Fe_2O_3 NFs (9.75 mg/mL) mixture and (B) Irradiated Ag_2S LNThs (0.5 mg/mL) + γ-Fe_2O_3 NFs (9.75 mg/mL) mixture.

(S7) Discussion of XANES and EXAFS

The possible presence of iron released into the Ag_2S LNThs was also studied with X-ray absorption spectroscopy (XAS) measurements at the Ag K-edge (25514 eV) (**Figure S7A**). X-ray absorption near edge structure (XANES) spectra for the Ag_2S LNThs and nanofluid without and upon irradiation show similar signal compared with Ag_2S reference. Only one slight shift towards larger energies of around 1.5 eV of nanofluid (with and without irradiation process) with respect to the Ag_2S is identified, which can be associated with an oxidation on the state of Ag ions or their coordination state (**Figure S7B**).[3, 4] A change of valence is discarded by extended X-ray absorption fine structure (EXAFS) because a Ag-O shell is not observed (**Figure S7C**). The presence of NFs in the Ag_2S LNThs resulted in a slight increase in the atomic coordination of the Ag-S distance (around 2.5 Å), which is maintained with the irradiation. Changes related to local structural disorder (Debye-Waller factor) are discarded through simulations (not shown). Specifically, at larger interatomic distances around 3.5-4 Å, related to Ag-Ag shells, a variation in the position and the intensity is detected in the irradiated sample. Since the mixture of Ag_2S with NFs has the only ion contribution of $Fe^{2+/3+}$, a possible explanation of EXAFS signal at those positions could be related to the incorporation of Fe in the structure Ag_2S or the formation of some compound with Ag-Fe interactions, where a larger contribution of Ag-Ag distance occurs.

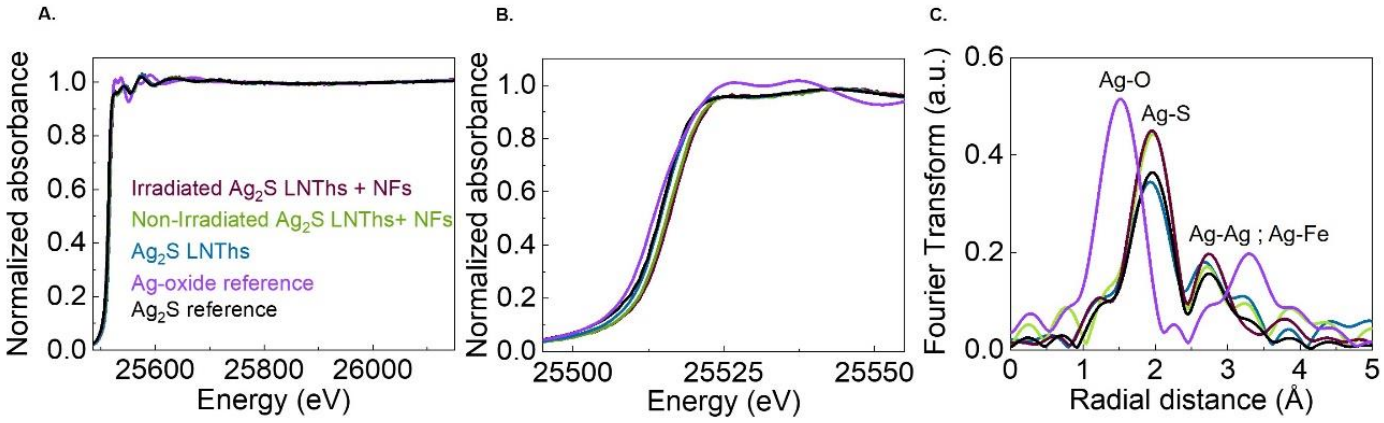

Figure S7. (A) XAS spectra at the Ag K-edge for Ag_2S LNThs and γ-Fe_2O_3 NFs mixtures, along Ag_2S and AgO references. (B) XANES part of the spectra. For the mixtures (with and without irradiation), there is slight shift in the absorption edge towards larger energies of around 1.5 eV with respect to the Ag_2S LNThs. (C) Fourier transform of EXAFS signal for different samples and references.

(S8) Datasets used to extract information of Figures 4B-E

Black arrows indicate the last measurement after 3 h of irradiation. The colored arrow indicates the increasing time of irradiation (t = 0, 5, 10, 15, 20, 30, 45, 60, 75, 90, 105, 120, 140, 160 and 180 min)

Effect of nanoflower concentration: Figure 4B

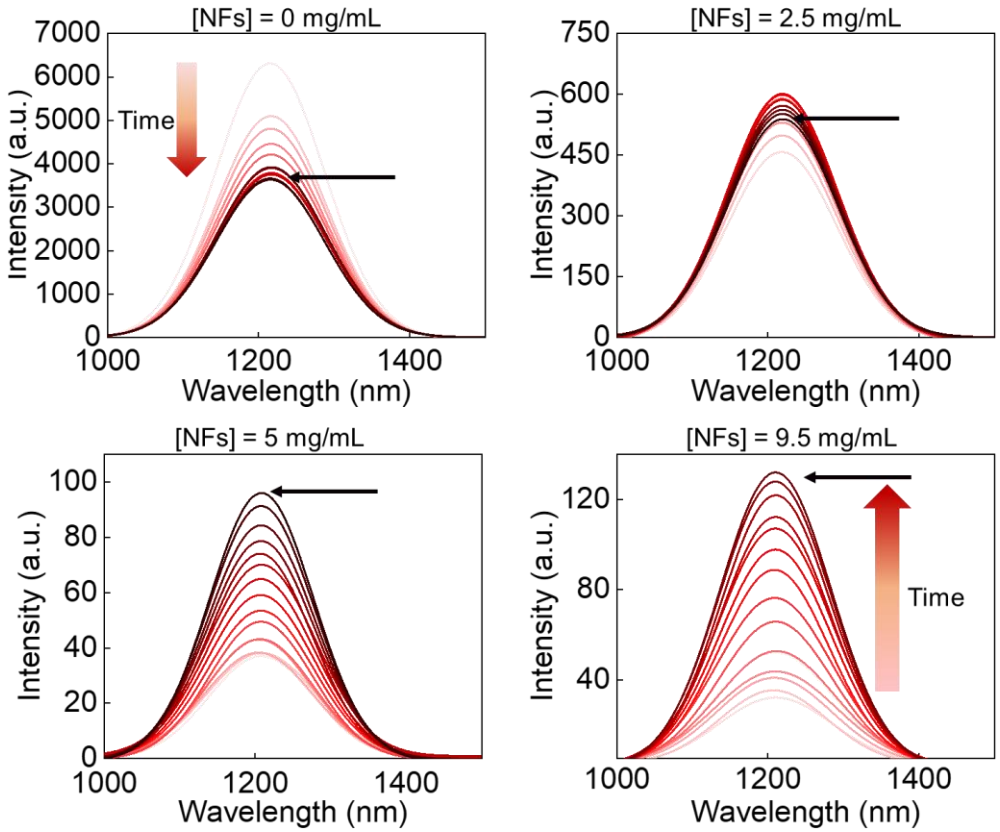

Figure S8A. Effect of NF concentration. Note that for 0 mg/mL the behavior of the LNThs is the expected: a decrease in intensity (quenching, indicating heating). Once the NFs are incorporated instead of an emission quenching, an intensity enhancement was observed.

Effect of laser power: Figure 4C

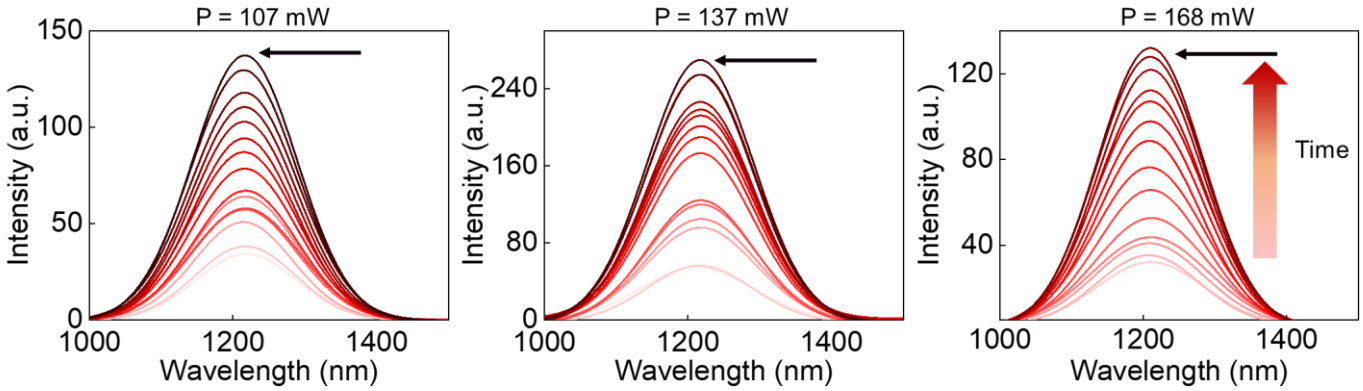

Figure S8B. Effect of laser power. The process is favored with increasing laser powers.

Effect of laser wavelength: Figure 4D

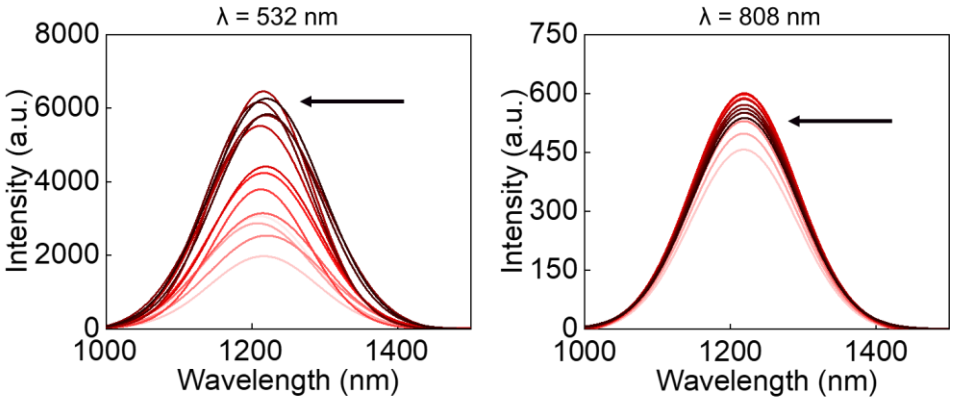

Figure S8C. Effect of laser wavelength. Under 532 nm irradiation (P = 28 mW) a greater enhancement is observed compared to the one obtained using an 808 nm laser (P = 168 mW).

Effect of nanofluid temperature: Figure 4E

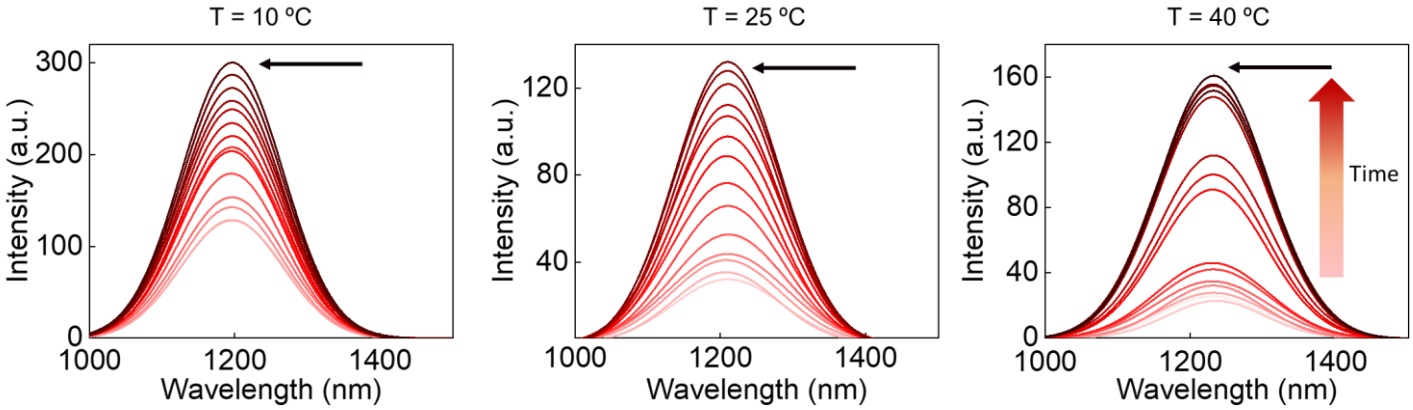

Figure S8D. Effect of nanofluid temperature. The process is favored when the external temperature is higher.

(III) References

1. I. Z. Gutierrez, C. Gerke, Y. Shen, E. Ximendes, M. M. Silvan, R. Marin, D. Jaque, O. G. Calderón, S. Melle and J. Rubio-Retama, *ACS Applied Materials Interfaces*, 2022, **14**, 4871-4881.
2. B. Ravel and M. Newville, *Journal of synchrotron radiation*, 2005, **12**, 537-541.
3. B. A. Manning, S. R. Kanel, E. Guzman, S. W. Brittle and I. E. Pavel, *Journal of Nanoparticle Research*, 2019, **21**, 1-14.
4. B. Kyffin, D. Pickup, G. Mountjoy, F. Foroutan, I. Abrahams and D. Carta, *The Journal of Physical Chemistry C*, 2021, **125**, 12256-12268.